Vol 451|21 February 2008|doi:10.1038/nature06668

ARTICLES

Phosphoinositide signalling links *O*-GlcNAc transferase to insulin resistance

Xiaoyong Yang[1], Pat P. Ongusaha[2], Philip D. Miles[3], Joyce C. Havstad[1], Fengxue Zhang[4], W. Venus So[5], Jeffrey E. Kudlow[4], Robert H. Michell[6], Jerrold M. Olefsky[3], Seth J. Field[3] & Ronald M. Evans[1]

Glucose flux through the hexosamine biosynthetic pathway leads to the post-translational modification of cytoplasmic and nuclear proteins by *O*-linked β-*N*-acetylglucosamine (*O*-GlcNAc). This tandem system serves as a nutrient sensor to couple systemic metabolic status to cellular regulation of signal transduction, transcription, and protein degradation. Here we show that *O*-GlcNAc transferase (OGT) harbours a previously unrecognized type of phosphoinositide-binding domain. After induction with insulin, phosphatidylinositol 3,4,5-trisphosphate recruits OGT from the nucleus to the plasma membrane, where the enzyme catalyses dynamic modification of the insulin signalling pathway by *O*-GlcNAc. This results in the alteration in phosphorylation of key signalling molecules and the attenuation of insulin signal transduction. Hepatic overexpression of OGT impairs the expression of insulin-responsive genes and causes insulin resistance and dyslipidaemia. These findings identify a molecular mechanism by which nutritional cues regulate insulin signalling through *O*-GlcNAc, and underscore the contribution of this modification to the aetiology of insulin resistance and type 2 diabetes.

The relentless progression of diabetes mellitus is rapidly becoming one of the principal threats to human health in the twenty-first century[1]. Nutrient excess and sedentary lifestyle are two of the major culprits fuelling the diabetes epidemic[2,3]. Type 2 diabetes results from a disruption of normal glucose homeostasis, primarily as a result of decreased peripheral insulin action coupled with relative insulin insufficiency[4,5]. However, the mechanisms by which excessive nutrients produce peripheral insulin resistance are not well understood.

Phosphatidylinositol 3,4,5-trisphosphate ($PI(3,4,5)P_3$) is a central mediator of insulin signalling[6–8]. On binding insulin, the insulin receptor (IR) catalyses tyrosine phosphorylation of the insulin receptor substrate (IRS) proteins, which results in the recruitment and activation of phosphatidylinositol-3-OH kinase (PI(3)K). The lipid product of PI(3)K, $PI(3,4,5)P_3$, recruits a subset of signalling proteins with pleckstrin homology (PH) domains, such as phosphoinositide-dependent kinase 1 (PDK1) and Akt, to the plasma membrane, where PDK1 induces the threonine phosphorylation and activation of Akt. Together these kinases initiate complex sets of transcriptional and post-transcriptional events that promote the synthesis and storage of carbohydrates, lipids and proteins and inhibit their degradation and release into the circulation[5].

Because sustained insulin action would be detrimental to physiological homeostasis, several feedback mechanisms have evolved to attenuate signalling[9]. Protein tyrosine phosphatases and phosphoinositide phosphatases exert inhibitory effects at defined sites in the proximal insulin signalling pathway[10,11]. Phosphorylation of IRS proteins by serine/threonine kinases is emerging as a mechanism for negative-feedback inhibition of insulin signalling and for cross-talk from other signalling pathways[12,13]. This is relevant because aberrant serine phosphorylation of IRS proteins is tightly linked to the aetiology of insulin resistance[13].

Glucose flux through the hexosamine biosynthetic pathway leads to the post-translational modification of cytoplasmic and nuclear proteins by *O*-GlcNAc[14,15]. OGT catalyses the attachment of *O*-GlcNAc to proteins, whereas *O*-GlcNAcase catalyses the sugar removal[16–18]. This dynamic and reversible modification is emerging as a key regulator of various cellular processes, such as signal transduction, transcription and proteasomal degradation[15,19–22]. Perturbations in protein *O*-GlcNAc modification are implicated in various human diseases including diabetes mellitus, neurodegeneration and cancer[23–31].

The end product of hexosamine biosynthesis, UDP-GlcNAc, donates the GlcNAc moiety for this modification[32]. The UDP-GlcNAc levels fluctuate with the availability of glucose, non-esterified fatty acids, uridine and the amino acid glutamine[15,33–35]. It has therefore been proposed that *O*-GlcNAc may serve as a nutrient sensor[36,37]. Our previous studies have defined nuclear *O*-GlcNAc as a negative regulator of transcription in response to steroid hormone signalling[20,38]. To gain insight into how cytoplasmic *O*-GlcNAc couples systemic metabolic status to the regulation of signal transduction, we explored the molecular basis on which *O*-GlcNAc regulates insulin signalling in response to glucose flux, and to understand the contribution of this nutrient sensor to the aetiology of insulin resistance.

OGT interacts with phosphoinositides

Because OGT shares homology with protein phosphatase 5, which exhibits affinity for lipids[39], we examined whether OGT could interact with lipids to act as an atypical lipid sensor. In a protein–lipid overlay assay, we found that OGT has affinity for a variety of PIP species (Fig. 1a). Deletion analysis mapped the PIP-binding region within amino-acid residues 958–1001 adjacent to the catalytic domain II at the carboxy terminus of OGT (Supplementary Fig. 1). In the blots with serial dilutions of diverse phospholipids, the full-length OGT binds most tightly with $PI(3,4,5)P_3$, whereas the deletion mutants (471C and 821C) that retain the C-terminal regions also

[1]Howard Hughes Medical Institute and Gene Expression Laboratory, The Salk Institute for Biological Studies, La Jolla, California 92037, USA. [2]Cutaneous Biology Research Center, Massachusetts General Hospital and Harvard Medical School, Charlestown, Massachusetts 02129, USA. [3]Department of Medicine, University of California, San Diego, La Jolla, California 92093, USA. [4]Department of Medicine, University of Alabama, Birmingham, Alabama 35294, USA. [5]Roche Group Research Information, Hoffmann-La Roche, Inc., Nutley, New Jersey 07110, USA. [6]School of Biosciences, University of Birmingham, Birmingham B15 2TT, UK.

show strong interaction with PI(4)P and PI(3,5)P_2, indicating that the N-terminal region renders OGT specific for PI(3,4,5)P_3 (Fig. 1b). To further characterize the PIP-binding domain in OGT, its primary sequence was interrogated against public databases including PROSITE, BLOCKS, ProDom, PRINTS, Pfam and SMART. We detected no homology between OGT and any known PIP-binding motifs. We therefore named this new class of motif the PPO (PIP-binding activity of OGT) domain.

Because acidic phosphate groups in PIPs are required for the interaction with OGT (Fig. 1a), we tested whether basic residues abundant in the PPO domain mediate this protein–lipid interaction. As shown in Fig. 1c and Supplementary Fig. 2, a double mutation of lysine residues to alanines (K981A/K982A) completely abolished the binding of the OGT(919C) fragment to PIPs, and K986A and K989A single mutations decreased lipid binding. In contrast, arginines 984 and 991 and lysine 1000 were dispensable for the PIP interaction (Supplementary Fig. 2). Thus, a cluster of lysine residues in the PPO domain are involved in the interaction with PIPs.

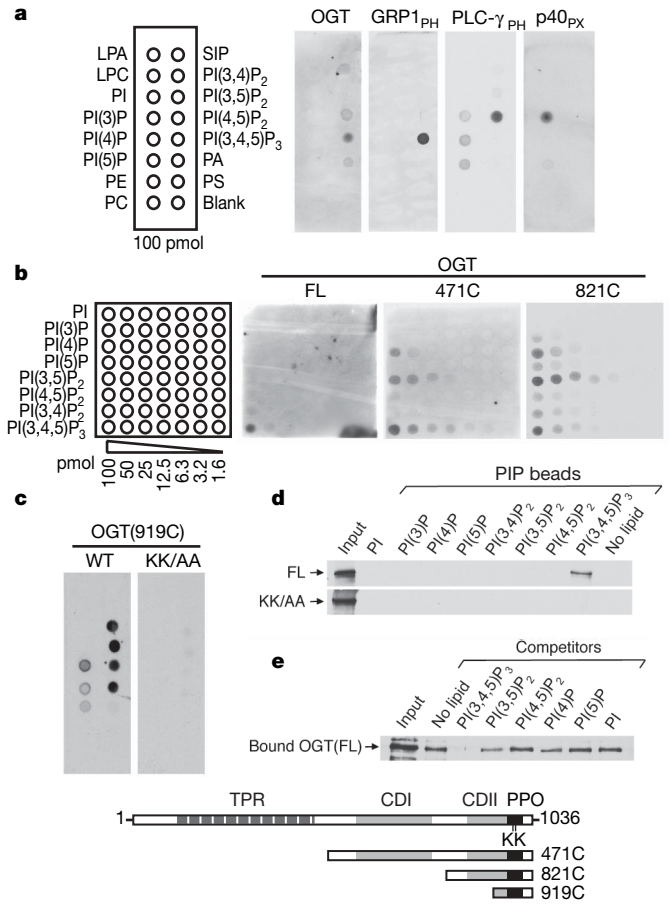

Figure 1 | OGT interacts with phosphoinositides. a, Binding of OGT to phospholipids immobilized on nitrocellulose membranes (PIP strips; Echelon Biosciences). Binding of the PH, PH and PX domains of GRP1, phospholipase Cγ (PLC-γ) and p40, respectively, to PIP strip lipid blots served as quality controls. Left, diagram of phospholipid species. LPA, lysophosphatidic acid; LPC, lysophosphatidylcholine; PE, phosphatidylethanolamine; PC, phosphatidylcholine; SIP, sphingosine 1-phosphate; PA, phosphatidic acid; PS, phosphatidylserine. **b**, Binding of full-length (FL) OGT and deletion mutants to lipid blots (PIP arrays; Echelon Biosciences). Left, diagram of phosphoinositide species and concentrations. **c**, Binding of OGT(919–1036) fragment to a lipid blot in the absence or presence of the KK/AA mutation. **d**, Pulling-down of full-length OGT without or with the KK/AA mutation by various phosphoinositide-coupled affinity beads (Echelon Biosciences). **e**, Pulling-down of full-length OGT by PI(3,4,5)P_3-coupled beads in the presence of various free phosphoinositides. Bottom, schematic representation of full-length OGT and various deletion mutants. TPR, tetratricopeptide repeats; CDI and CDII, catalytic domains I and II; PPO, PIP-binding domain.

We validated these results by an independent method for detecting protein–lipid interactions. Among different PIP-coupled affinity beads, the full-length OGT bound specifically to beads bearing PI(3,4,5)P_3, which was abolished by the (K981A/K982A) mutation (Fig. 1d). The addition of free PI(3,4,5)P_3 effectively displaced OGT from PI(3,4,5)P_3 beads, but other free PIPs had no effect (Fig. 1e). These results confirmed that OGT can bind selectively to PI(3,4,5)P_3 through the PPO domain.

PI(3,4,5)P_3 mediates OGT translocation

The ability of OGT to bind PI(3,4,5)P_3 *in vitro* raises the question of whether they functionally interact *in vivo*. In an OGT activity assay, none of the PIP species measurably affected the ability of OGT to modify a protein substrate, p62, arguing against a role for PIPs in regulating the catalytic activity of the enzyme (Supplementary Fig. 4).

Activation of PI(3)K leads to the accumulation of PI(3,4,5)P_3 at the plasma membrane in response to various extracellular signals such as insulin. The interaction between OGT and PI(3,4,5)P_3 prompted us to examine the subcellular localization of OGT on PI(3)K signalling. As shown in Fig. 2a and Supplementary Movies 1 and 3, green fluorescent protein (GFP)–OGT translocated rapidly to the plasma membrane within 90 s of stimulation with serum in live cells. Pretreatment with the PI(3)K inhibitor wortmannin completely blocked GFP–OGT translocation in response to serum (Supplementary Movie 2). Similarly, the addition of wortmannin after stimulation with serum led to rapid dissociation from the plasma membrane (within 3 min), indicating that association with the plasma membrane was dependent on sustained PI(3)K activity (Fig. 2a and Supplementary Movie 3).

We compared the subcellular localization of GFP–OGT with that of a biosensor for PI(3,4,5)P_3, the Akt PH domain fused to a red fluorescent protein (HcRed–Akt_{PH}). Both translocated to and co-localized at the plasma membrane within 30 min after stimulation with serum, indicating their recruitment to the plasma membrane by a common mechanism (Fig. 2b). For both GFP–OGT and HcRed–Akt_{PH}, their associations with the plasma membrane were observed in more than 80% of cells at 5 min after treatment with serum, and the numbers were markedly reduced at 60 min (Fig. 2c). As a control, the localization of GFP was unaffected by serum (Supplementary Fig. 5).

We next examined whether activated PI(3)K is sufficient to drive GFP–OGT redistribution. Expression of a constitutively active PI(3)K led to translocation of GFP–OGT to the plasma membrane even under conditions of serum starvation (Supplementary Movie 4). Again, treatment with wortmannin led to rapid dissociation from the plasma membrane. This result was further supported by our subcellular fractionation experiment, showing that the constitutively active PI(3)K, but not a catalytically dead one, also triggered GFP–OGT accumulation at the plasma membrane (Fig. 2d). As the controls, GFP, the plasma membrane marker Na/K ATPase and the cytoplasmic marker β-actin were not affected (Fig. 2d). Activated PI(3)K is therefore both necessary and sufficient to drive the translocation of GFP–OGT to the plasma membrane.

We examined the subcellular localization of endogenous OGT and Akt. Immunostaining revealed that, similarly to the GFP-tagged proteins, endogenous OGT and Akt were co-localized at the plasma membrane after serum treatment (Supplementary Fig. 6). Consistent with this observation, subcellular fractionation showed that endogenous OGT and Akt accumulated in the plasma membrane fraction in response to insulin but not in the presence of wortmannin (Fig. 2e). The localization of endogenous OGT is therefore regulated by PI(3)K.

Inhibition of PI(3,4,5)P_3 production by PTEN (phosphatase and tensin homolog (mutated in multiple advanced cancers 1)) also markedly decreased the association of OGT with the plasma

membrane (Supplementary Fig. 7), further supporting the notion that PI(3,4,5)P_3 recruits OGT to the plasma membrane on insulin signalling.

Finally, we tested whether the K981A/K982A point mutation that abolishes interaction with PI(3,4,5)P_3 *in vitro* also affected the response of OGT to PI(3,4,5)P_3 *in vivo*. Indeed, the K981A/K982A mutant did not translocate to the plasma membrane in response to stimulation with serum or in response to the expression of the constitutively active PI(3)K (Fig. 2f, and Supplementary Movies 5 and 6). Taken together, these results indicate that OGT is a target of PI(3,4,5)P_3 *in vivo*.

O-GlcNAc regulation of insulin signalling

We next sought to dissect events downstream of insulin-stimulated recruitment of OGT to the plasma membrane. In general, the magnitude of *O*-GlcNAc modification of intracellular proteins correlates with extracellular glucose levels[34,35]. We observed that the exposure of 3T3-L1 adipocytes to either high glucose (30 mM) or an *O*-GlcNAcase inhibitor (PUGNAc)—two approaches that increase protein *O*-GlcNAc concentrations—inhibited insulin-stimulated phosphorylation of Akt specifically at Thr 308 but not at another critical phosphorylation site (Ser 473), which is consistent with previous reports[30,40] (Fig. 3a, b). In contrast, phosphorylation of PDK1 at Ser 241 was not affected (Fig. 3a, b). Glucose deprivation had no immediate effect on the phosphorylation of these signalling components (Fig. 3a). We observed that exposing the cells to various concentrations of glucose and insulin did not alter global concentrations of *O*-GlcNAc and phosphotyrosine but rather that of specific proteins (Supplementary Fig. 8).

Concurrent with the decrease in phosphorylation of Akt Thr 308, the increase in intracellular *O*-GlcNAc levels brought about by high concentrations of glucose or by PUGNAc inhibited Akt kinase activity (Fig. 3d). Under the same conditions, extracellular signal-regulated kinase (ERK)1/2 kinase activity remained unchanged (Fig. 3d).

In addition to suppressing Akt phosphorylation and activity, PUGNAc enhanced IRS1 phosphorylation at Ser 307 and Ser 632/635 (Fig. 3b), sites previously shown to mediate the attenuation of insulin signalling[12,13]. In line with these results, adenovirus-mediated overexpression of OGT (Ad-OGT) decreased the phosphorylation of

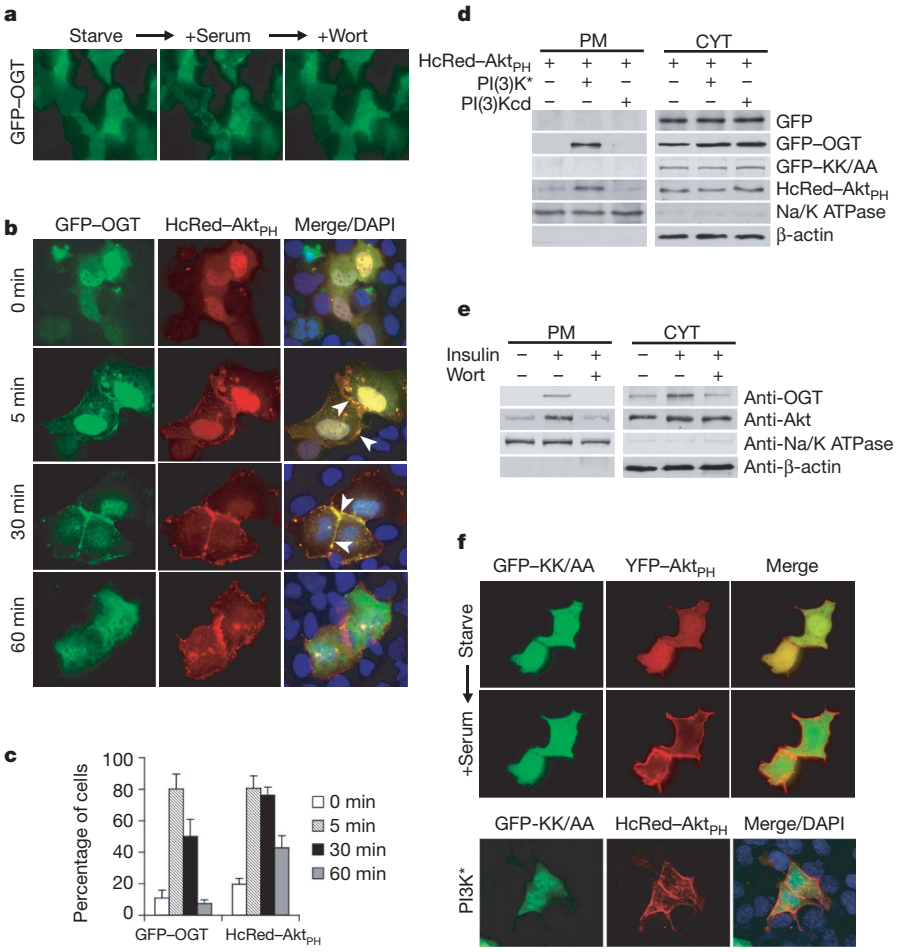

Figure 2 | Phosphoinositide signalling mediates OGT translocation. **a**, Live images of COS-7 cells transfected with the GFP–OGT expression vector, serum-starved overnight and treated with 10% serum and then 100 nM wortmannin (Wort) (from Supplementary Movie 3). **b**, Fluorescent images of fixed COS-7 cells that were co-transfected with the GFP–OGT and HcRed–Akt$_{PH}$ expression vectors followed by treatment with serum for the indicated periods. Right panels, images merged with 4,6-diamidino-2-phenylindole (DAPI) staining of nuclei. Arrows indicate co-localization of GFP–OGT and HcRed–Akt$_{PH}$ on plasma membrane. **c**, Quantification of cells that displayed the plasma membrane localization of GFP–OGT or HcRed–Akt$_{PH}$ after serum treatment for the indicated periods. Error bars show s.e.m. **d**, Immunoblot analysis of subcellular fractionations using anti-GFP, anti-HcRed, anti-Na/K ATPase and anti-β-actin antibodies after COS-7 cells had been transfected with the GFP, GFP–OGT or GFP–KK/AA vector plus the indicated expression vectors. PM, plasma membrane; CYT, cytosol. **e**, Immunoblot analysis of endogenous OGT and Akt in subcellular fractions of 3T3-A14 cells treated with 100 nM insulin minus or plus 100 nM Wort for 30 min. **f**, Top: live images of COS-7 cells co-transfected with the GFP–OGT (KK/AA) mutant and yellow fluorescent protein (YFP)–Akt$_{PH}$, serum-starved overnight and treated with 10% serum (from Supplementary Movie 5). Bottom: images of fixed COS-7 cells co-transfected with the vectors expressing GFP–KK/AA, HcRed–Akt$_{PH}$ and constitutively active PI(3)K (PI(3)K*).

Akt at Thr 308 and its kinase activity, and increased phosphorylation of IRS1 at Ser 307 and Ser 632/635 (Fig. 3c and Supplementary Fig. 9), providing direct evidence for the regulation of the serine/threonine phosphorylation of Akt and IRS1 by *O*-GlcNAc. This regulatory mechanism is not adipocyte-specific, because PUGNAc and Ad-OGT also modulated the phosphorylation of Thr 308 of Akt and Ser 632/635 of IRS1 in Fao hepatoma cells in a PPO-domain-dependent manner (Supplementary Figs 10 and 11). An alteration in *O*-GlcNAc levels had no significant effect on tyrosine phosphorylation of purified IR-β and whole-cell proteins (Fig. 3c, e).

Next we assessed direct targets of OGT in the insulin signalling pathway[41,42]. We found that IR-β and IRS1 were modified by *O*-GlcNAc on stimulation with insulin (Supplementary Fig. 12). Glycosylation of IR-β and IRS1 was highly dynamic, reaching maximum levels at 30 min and declining quickly within 1 h. In contrast, tyrosine phosphorylation of the two proteins was initiated earlier than their glycosylation but was prolonged over 8 h (Fig. 3f). Besides IRS1, other insulin signalling components, including Akt, PDK1 and the p110α subunit of PI(3)K, were detectable in anti-*O*-GlcNAc immunoprecipitates, in which insulin and PUGNAc treatments increased the amounts of glycosylated IRS1 and Akt but not those of PDK1 and p110α (Supplementary Fig. 13). A reciprocal experiment showed that insulin and PUGNAc also increased the glycosylation levels of Akt immunoprecipitates, which is in agreement with a previous report confirming that Akt itself is dynamically modified by *O*-GlcNAc[42] (Supplementary Fig. 14). Taken together, these results indicate that the insulin-induced recruitment of OGT to the plasma membrane imposes *O*-GlcNAc modification on specific signalling components, which in turn influences their phosphorylation level and activity. The half-life of protein phosphorylation in the insulin pathway seems not be affected by *O*-GlcNAc (data not shown).

The ability of *O*-GlcNAc to inhibit Akt phosphorylation and enhance IRS1 serine phosphorylation indicates adverse effects of this modification on insulin signalling. Indeed, increased *O*-GlcNAc modification by PUGNAc inhibited insulin-stimulated glucose transport in 3T3-L1 adipocyte (Supplementary Fig. 15), suggesting that *O*-GlcNAc is involved in attenuation of insulin signalling.

OGT–lipid interaction mediates insulin resistance

Insulin is a pivotal regulator of carbohydrate and lipid metabolism. To investigate whether OGT modulates insulin signalling in a physiological context, we conducted glucose tolerance tests on C57BL/6J mice with adenoviral delivery of wild-type OGT (Ad-OGT) and the PIP-binding-deficient mutant (Ad-KK/AA) expression constructs to the liver. Glucose excursion curves were similar in Ad-OGT and Ad-KK/AA mice compared with mice transduced with the Ad-GFP control (Fig. 4a). However, Ad-OGT mice had higher levels of plasma insulin and C-peptide than Ad-KK/AA and control mice at 20 min after the glucose challenge (Supplementary Figs 16 and 17), indicating the possible existence of peripheral insulin resistance in Ad-OGT mice with a compensatory increase in insulin release. Indeed, during insulin tolerance tests, Ad-OGT mice showed an impaired decrease in blood glucose at 40 min compared with Ad-KK/AA and control mice (Fig. 4b). Hyperinsulinaemic–euglycaemic glucose clamp experiments showed that the insulin-stimulated glucose disposal rate was similar in Ad-OGT and control mice, indicating that Ad-OGT might not affect the sensitivity of muscle and adipose tissue, the major sites of glucose disposal, to insulin (Fig. 4c). In contract, basal glucose turnover was decreased and the ability of insulin to suppress hepatic glucose production was attenuated in Ad-OGT mice, demonstrating the presence of hepatic insulin resistance (Fig. 4d, e).

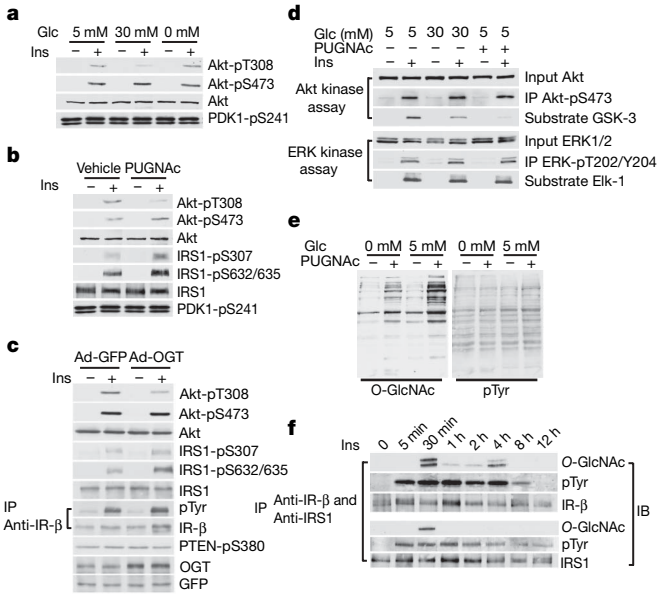

Figure 3 | *O*-GlcNAc dynamically regulates insulin signalling pathway. **a**, **b**, Immunoblot analysis of phosphorylation states and total amounts of the indicated proteins in differentiated 3T3-L1 cells. Cells were incubated for 16 h with various concentrations of glucose (Glc) (**a**) or with 5 mM glucose plus 100 μM PUGNAc (**b**), followed by insulin (Ins) treatment for 30 min. **c**, Immunoblot assay of cell extracts after adenoviral expression of GFP or OGT. Tyrosine phosphorylation (pTyr) was assessed in anti-IR-β immunoprecipitates. IP, immunoprecipitation. **d**, Kinase assays showing the activity of immunoprecipitated phospho-Akt (Ser 473) in phosphorylating the GSK-3α/β crosstide sequence (CGPKGPGRRGRRRTSSFAEG) and the activity of immunoprecipitated phospho-ERK1/2 (Thr 202/Tyr 204) in phosphorylating Elk-1 on the treatments as indicated. **e**, Immunoblot analysis of whole-cell lysates with anti-*O*-GlcNAc antibody (RL2) or anti-phosphotyrosine antibody (4G10) after the indicated treatments for 16 h. **f**, Time course of glycosylation and phosphorylation of IR-β and IRS1. Whole-cell lysates were immunoprecipitated with a mixture of anti-IR-β and anti-IRS1 antibodies, and then immunoblotted (IB) with anti-*O*-GlcNAc antibody (RL2) or anti-phosphotyrosine antibody (4G10).

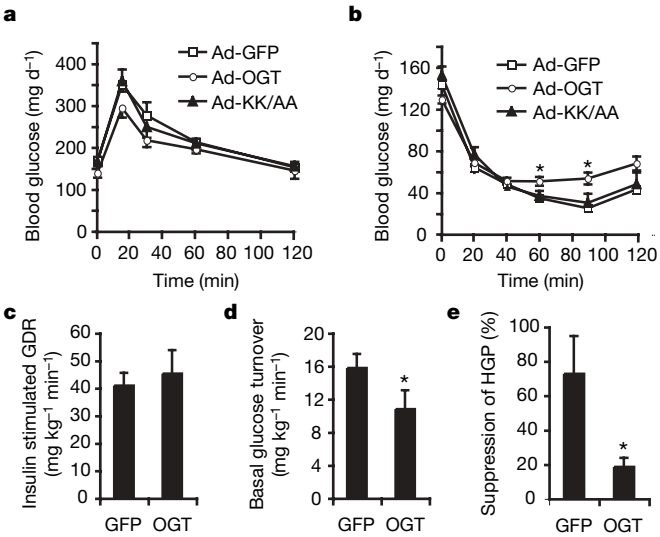

Figure 4 | Hepatic overexpression of OGT produces insulin resistance. **a**, **b**, Glucose (**a**) and insulin (**b**) tolerance tests in 12-week-old C57BL/6J male mice infected with adenovirus expressing GFP or the wild-type or KK/AA mutant of OGT ($n = 6$). Glucose (1.5 g kg^{-1} body weight) (**a**) or insulin (1.5 U kg^{-1} body weight) (**b**) were injected intraperitoneally (i.p.) 6 h after food removal. Asterisk, $P < 0.05$ versus GFP mice. **c**–**e**, Hyperinsulinaemic–euglycaemic glucose clamp studies of 16-week-old mice infected with GFP or OGT adenovirus. Basal glucose turnover ($n = 8$) (**d**), insulin-stimulated glucose disposal rate (GDR) ($n = 7$) (**c**) and percentage suppression of hepatic glucose production (HGP) ($n = 9$) (**e**) were measured. Asterisk, $P < 0.05$ versus GFP mice. Error bars show s.e.m.

Insulin suppresses hepatic glucose production by inhibiting gluconeogenesis and promoting glycolysis and glycogen synthesis. The delivery of Ad-OGT to the liver increased the expression of gluconeogenic genes (those encoding phosphoenolpyruvate carboxykinase and glucose-6-phosphatase) and decreased the expression of glycolytic genes (those encoding glucokinase and glyceraldehyde-3-phosphate dehydrogenase), and these changes were not seen in the mice expressing the KK/AA mutant (Fig. 5a). Moreover, the wild-type Ad-OGT, but not the mutant, decreased glycogen content in the liver, indicating an inhibitory effect of OGT on glycogen synthesis (Fig. 5c).

Insulin promotes lipid synthesis by inducing the expression of lipogenic genes. Ad-OGT expression repressed the level of sterol regulatory element-binding protein-1c (*SREBP-1c*), known as the master regulator of lipogenesis, as well as its target genes including those encoding acetyl-CoA carboxylase 1 (*ACC1*), fatty acid synthase (*FAS*) and stearoyl-CoA desaturase 1 (*SCD1*) (Fig. 5b). This inhibitory effect was abrogated by the KK/AA mutation in OGT (Fig. 5b). The mRNA levels of the genes involved in fatty acid oxidation (those encoding peroxisome-proliferator-activated receptor-α, medium-chain acyl-CoA dehydrogenase and carnitine palmitoyltransferase 1A) and lipid transport (those encoding ATP binding cassette transporters A1, G5 and G8, and apolipoprotein A-I) were unchanged (data not shown).

Despite the decrease in lipogenic gene expression in the liver, Ad-OGT mice showed increased levels of plasma triacylglycerols and cholesterol in comparison with Ad-GFP and Ad-KK/AA mice (Fig. 5d, e). These results may be associated with repression of the gene encoding Insig-1, a negative regulator of lipid synthesis, by Ad-OGT (Fig. 5b). The concentrations of hepatic triacylglycerol, plasma non-esterified fatty acids, leptin, adiponectin and resistin were similar in the three groups (data not shown).

Our results reveal that hepatic overexpression of OGT impairs the expression of insulin-responsive genes and perturbs glucose and lipid homeostasis in a PPO-domain-dependent manner. Because the KK/AA mutation does not affect the catalytic activity of OGT (Supplementary Fig. 18), these phenotypes are intrinsically dependent on the PIP-binding activity of the enzyme. To ascertain whether this is attributable to defective insulin signal transduction, we examined the phosphorylation state of the insulin pathway. Consistent with our observations in 3T3-L1 and Fao cells (Fig. 3c and Supplementary Fig. 11), Ad-OGT increased insulin-stimulated IRS1 phosphorylation at Ser 307 and Ser 632/635 and decreased Akt phosphorylation at Thr 308 in the liver, whereas Ad-KK/AA had no effect (Fig. 5f). Ser 9 phosphorylation of hepatic glycogen synthase kinase (GSK)-3β was also decreased, which may account for the inhibitory effect of Ad-OGT on glycogen synthesis. In accord with a lack of adenoviral infection in muscle and adipose tissue of Ad-OGT mice, their insulin signalling cascades remained intact (Supplementary Figs 19–21). This leads us to conclude that Ad-OGT induces insulin resistance and dyslipidaemia by PIP-dependent perturbation of insulin signalling.

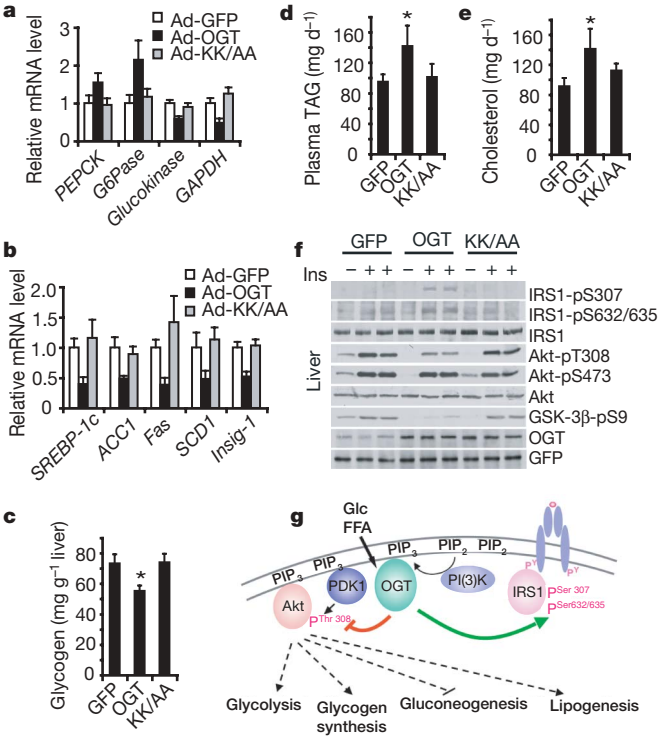

Figure 5 | OGT overexpression causes phosphoinositide-dependent perturbation of insulin signalling. **a**, **b**, Quantitative PCR analysis of gene expression with the use of liver RNA from 6-h-fasted mice infected with the indicated viruses ($n = 4$–6). PEPCK, phosphoenolpyruvate carboxykinase; G6Pase, glucose-6-phosphatase; GAPDH, glyceraldehyde-3-phosphate dehydrogenase. **c**–**e**, Liver glycogen contents, plasma triacylglycerol (TAG) and cholesterol levels in 6-h-fasted mice at 7 days after adenoviral infection ($n = 5$–6). Asterisk, $P < 0.05$ versus GFP mice. Error bars show s.e.m. **f**, Immunoblot analysis of liver extracts from adenovirus-infected mice injected intraperitoneally with insulin (3 U kg^{-1} body weight) or vehicle for 15 min. **g**, Model showing that, under normal physiological conditions, PI(3,4,5)P_3 recruits OGT to the plasma membrane in 'phase II', where OGT attenuates insulin signalling by inhibiting phosphorylation at Thr 308 of Akt and promoting IRS1 serine phosphorylation. Excessive quantities of nutrients such as glucose and non-esterified fatty acids aberrantly elevate *O*-GlcNAc levels, thereby impairing insulin action on carbohydrate and lipid metabolism.

Discussion

Mounting evidence points to pivotal roles of *O*-GlcNAc modification in regulating diverse functions of nuclear and cytoplasmic proteins[15,37]. Our studies provide the first evidence that this modification mediates critical signalling events at the plasma membrane and identify a previously unrecognized type of PI(3,4,5)P_3-binding domain as a critical modulator of this process. Thus, the PPO domain of OGT opens up a target through which phosphoinositide signalling can directly modulate hexosamine signalling and sensitivity.

Activation followed by termination of signal transduction is essential for all signalling pathways. Our studies reveal a new strategy for the attenuation of insulin signal transduction. Insulin stimulates the production of PI(3,4,5)P_3 at the plasma membrane, where the lipid recruits PDK1 and Akt to initiate early signalling cascades. As we now show, PI(3,4,5)P_3 also recruits OGT to the plasma membrane, where the enzyme acts in a 'phase II' pathway to catalyse dynamic modification of Akt, IRS1 and probably other signalling molecules by *O*-GlcNAc. This inhibits the phosphorylation of Akt at Thr 308 and promotes the phosphorylation of IRS1 at multiple serine residues. As a consequence, OGT modulates the termination (but not the activation) of insulin signalling, hence the term phase II regulation (Fig. 5g). Because *O*-GlcNAc seems not to affect the activities of PI(3)K and PDK1 (X.Y. and R.M.E., unpublished observations), OGT may modulate specific branches in the insulin signalling network.

O-GlcNAc is a putative cellular sensor for systemic metabolic status. Our studies indicate how nutritional cues may regulate insulin signalling through *O*-GlcNAc. Under normal physiological conditions, balanced *O*-GlcNAc levels may confer optimal kinetics of insulin signal transduction. Nutrient excess would lead to aberrant elevation in *O*-GlcNAc levels, which in turn compromise the efficiency of insulin signalling (Fig. 5g). Abnormal *O*-GlcNAc modification of the insulin signalling pathway may therefore contribute to the pathophysiology of insulin resistance, obesity and type 2 diabetes.

METHODS SUMMARY

Protein–lipid overlay assays were performed in accordance with the manufacturer's protocols. Cells were cultured in DMEM medium with 10% FBS except that Fao hepatoma cells were maintained in RPMI 1640 with 10% FBS. 3T3-L1 cell differentiation was induced by an insulin/dexamethasone/isobutylmethyl xanthine cocktail. 3T3-A14 and COS-7 cells were transfected with Transfectin and FuGENE6, respectively. Treatments with various concentrations of glucose and 100 μM PUGNAc were performed in 0.5% BSA for 16 h, followed by stimulation with 10% FBS or 100 nM insulin. Microscopy was performed in fixed or live cells expressing fluorescent fusion proteins. Whole-cell lysates were prepared in RIPA buffer for immunoprecipitation and immunoblotting analyses. C57BL/6J mice were infected with recombinant adenoviruses with the use of systemic injection into the tail vein. Four to six days after viral infection, glucose and insulin tolerance tests were performed in mice that had been fasted for 6 h. After seven days, blood and tissues were collected from 6-h-fasted mice for the measurement of metabolic parameters, quantitative PCR and protein phosphorylation analyses.

Full Methods and any associated references are available in the online version of the paper at www.nature.com/nature.

Received 6 October 2007; accepted 7 January 2008.

1. Zimmet, P., Alberti, K. G. & Shaw, J. Global and societal implications of the diabetes epidemic. *Nature* **414,** 782–787 (2001).
2. Spiegelman, B. M. & Flier, J. S. Obesity and the regulation of energy balance. *Cell* **104,** 531–543 (2001).
3. Lazar, M. A. How obesity causes diabetes: not a tall tale. *Science* **307,** 373–375 (2005).
4. Taylor, S. I. Deconstructing type 2 diabetes. *Cell* **97,** 9–12 (1999).
5. Saltiel, A. R. & Kahn, C. R. Insulin signalling and the regulation of glucose and lipid metabolism. *Nature* **414,** 799–806 (2001).
6. Cantley, L. C. The phosphoinositide 3-kinase pathway. *Science* **296,** 1655–1657 (2002).
7. Shepherd, P. R., Withers, D. J. & Siddle, K. Phosphoinositide 3-kinase: the key switch mechanism in insulin signalling. *Biochem. J.* **333,** 471–490 (1998).
8. Hawkins, P. T., Anderson, K. E., Davidson, K. & Stephens, L. R. Signalling through Class I PI3Ks in mammalian cells. *Biochem. Soc. Trans.* **34,** 647–662 (2006).
9. Saltiel, A. R. & Pessin, J. E. Insulin signaling pathways in time and space. *Trends Cell Biol.* **12,** 65–71 (2002).
10. Asante-Appiah, E. & Kennedy, B. P. Protein tyrosine phosphatases: the quest for negative regulators of insulin action. *Am. J. Physiol. Endocrinol. Metab.* **284,** E663–E670 (2003).
11. Lazar, D. F. & Saltiel, A. R. Lipid phosphatases as drug discovery targets for type 2 diabetes. *Nature Rev. Drug Discov.* **5,** 333–342 (2006).
12. Zick, Y. Ser/Thr phosphorylation of IRS proteins: a molecular basis for insulin resistance. *Sci. STKE* **2005,** pe4 (2005).
13. White, M. F. IRS proteins and the common path to diabetes. *Am. J. Physiol. Endocrinol. Metab.* **283,** E413–E422 (2002).
14. Torres, C. R. & Hart, G. W. Topography and polypeptide distribution of terminal N-acetylglucosamine residues on the surfaces of intact lymphocytes. Evidence for O-linked GlcNAc. *J. Biol. Chem.* **259,** 3308–3317 (1984).
15. Love, D. C. & Hanover, J. A. The hexosamine signaling pathway: deciphering the 'O-GlcNAc code'. *Sci. STKE* **2005,** re13 (2005).
16. Gao, Y., Wells, L., Comer, F. I., Parker, G. J. & Hart, G. W. Dynamic O-glycosylation of nuclear and cytosolic proteins: cloning and characterization of a neutral, cytosolic β-N-acetylglucosaminidase from human brain. *J. Biol. Chem.* **276,** 9838–9845 (2001).
17. Kreppel, L. K., Blomberg, M. A. & Hart, G. W. Dynamic glycosylation of nuclear and cytosolic proteins. Cloning and characterization of a unique O-GlcNAc transferase with multiple tetratricopeptide repeats. *J. Biol. Chem.* **272,** 9308–9315 (1997).
18. Toleman, C., Paterson, A. J., Whisenhunt, T. R. & Kudlow, J. E. Characterization of the histone acetyltransferase (HAT) domain of a bifunctional protein with activable O-GlcNAcase and HAT activities. *J. Biol. Chem.* **279,** 53665–53673 (2004).
19. Yang, X. *et al.* O-linkage of N-acetylglucosamine to Sp1 activation domain inhibits its transcriptional capability. *Proc. Natl Acad. Sci. USA* **98,** 6611–6616 (2001).
20. Yang, X., Zhang, F. & Kudlow, J. E. Recruitment of O-GlcNAc transferase to promoters by corepressor mSin3A: coupling protein O-GlcNAcylation to transcriptional repression. *Cell* **110,** 69–80 (2002).
21. Zhang, F. *et al.* O-GlcNAc modification is an endogenous inhibitor of the proteasome. *Cell* **115,** 715–725 (2003).
22. Wells, L., Vosseller, K. & Hart, G. W. Glycosylation of nucleocytoplasmic proteins: signal transduction and O-GlcNAc. *Science* **291,** 2376–2378 (2001).
23. Buse, M. G. Hexosamines, insulin resistance, and the complications of diabetes: current status. *Am. J. Physiol. Endocrinol. Metab.* **290,** E1–E8 (2006).
24. Musicki, B., Kramer, M. F., Becker, R. E. & Burnett, A. L. Inactivation of phosphorylated endothelial nitric oxide synthase (Ser-1177) by O-GlcNAc in diabetes-associated erectile dysfunction. *Proc. Natl Acad. Sci. USA* **102,** 11870–11875 (2005).
25. Hanover, J. A. *et al.* A *Caenorhabditis elegans* model of insulin resistance: altered macronutrient storage and dauer formation in an OGT-1 knockout. *Proc. Natl Acad. Sci. USA* **102,** 11266–11271 (2005).
26. Lehman, D. M. *et al.* A single nucleotide polymorphism in MGEA5 encoding O-GlcNAc-selective N-acetyl-β-D glucosaminidase is associated with type 2 diabetes in Mexican Americans. *Diabetes* **54,** 1214–1221 (2005).
27. Majumdar, G. *et al.* Insulin stimulates and diabetes inhibits O-linked N-acetylglucosamine transferase and O-glycosylation of Sp1. *Diabetes* **53,** 3184–3192 (2004).
28. Konrad, R. J. & Kudlow, J. E. The role of O-linked protein glycosylation in beta-cell dysfunction. *Int. J. Mol. Med.* **10,** 535–539 (2002).
29. McClain, D. A. *et al.* Altered glycan-dependent signaling induces insulin resistance and hyperleptinemia. *Proc. Natl Acad. Sci. USA* **99,** 10695–10699 (2002).
30. Vosseller, K., Wells, L., Lane, M. D. & Hart, G. W. Elevated nucleocytoplasmic glycosylation by O-GlcNAc results in insulin resistance associated with defects in Akt activation in 3T3–L1 adipocytes. *Proc. Natl Acad. Sci. USA* **99,** 5313–5318 (2002).
31. Roos, M. D. *et al.* Streptozotocin, an analog of N-acetylglucosamine, blocks the removal of O-GlcNAc from intracellular proteins. *Proc. Assoc. Am. Physicians* **110,** 422–432 (1998).
32. Haltiwanger, R. S., Holt, G. D. & Hart, G. W. Enzymatic addition of O-GlcNAc to nuclear and cytoplasmic proteins. Identification of a uridine diphospho-N-acetylglucosamine:peptide β-N-acetylglucosaminyltransferase. *J. Biol. Chem.* **265,** 2563–2568 (1990).
33. Wang, J., Liu, R., Hawkins, M., Barzilai, N. & Rossetti, L. A nutrient-sensing pathway regulates leptin gene expression in muscle and fat. *Nature* **393,** 684–688 (1998).
34. Liu, K., Paterson, A. J., Chin, E. & Kudlow, J. E. Glucose stimulates protein modification by O-linked GlcNAc in pancreatic beta cells: linkage of O-linked GlcNAc to beta cell death. *Proc. Natl Acad. Sci. USA* **97,** 2820–2825 (2000).
35. Yki-Jarvinen, H., Virkamaki, A., Daniels, M. C., McClain, D. & Gottschalk, W. K. Insulin and glucosamine infusions increase O-linked N-acetyl-glucosamine in skeletal muscle proteins *in vivo*. *Metabolism* **47,** 449–455 (1998).
36. Wells, L., Vosseller, K. & Hart, G. W. A role for N-acetylglucosamine as a nutrient sensor and mediator of insulin resistance. *Cell. Mol. Life Sci.* **60,** 222–228 (2003).
37. Zachara, N. E. & Hart, G. W. O-GlcNAc a sensor of cellular state: the role of nucleocytoplasmic glycosylation in modulating cellular function in response to nutrition and stress. *Biochim. Biophys. Acta* **1673,** 13–28 (2004).
38. Whisenhunt, T. R. *et al.* Disrupting the enzyme complex regulating O-GlcNAcylation blocks signaling and development. *Glycobiology* **16,** 551–563 (2006).
39. Chen, M. X. & Cohen, P. T. Activation of protein phosphatase 5 by limited proteolysis or the binding of polyunsaturated fatty acids to the TPR domain. *FEBS Lett.* **400,** 136–140 (1997).
40. Arias, E. B., Kim, J. & Cartee, G. D. Prolonged incubation in PUGNAc results in increased protein O-linked glycosylation and insulin resistance in rat skeletal muscle. *Diabetes* **53,** 921–930 (2004).
41. D'Alessandris, C. *et al.* Increased O-glycosylation of insulin signaling proteins results in their impaired activation and enhanced susceptibility to apoptosis in pancreatic beta-cells. *FASEB J.* **18,** 959–961 (2004).
42. Park, S. Y., Ryu, J. & Lee, W. O-GlcNAc modification on IRS-1 and Akt2 by PUGNAc inhibits their phosphorylation and induces insulin resistance in rat primary adipocytes. *Exp. Mol. Med.* **37,** 220–229 (2005).

Supplementary Information is linked to the online version of the paper at www.nature.com/nature.

Acknowledgements We thank T. Hunter, B. Burgering, J. Yuan and O. Gozani for providing reagents; R. Shaw for advice; R. Shaw, S. Dove and H. Cho for critical reading of the manuscript; Z. Wu for help with statistical analysis; M. Nelson and K. Kawamura for technical assistance; and L. Ong and S. Ganley for administrative assistance. X.Y. is the recipient of a Ruth L. Kirschstein National Research Service Award Individual Fellowship. R.M.E. is an Investigator of the Howard Hughes Medical Institute at the Salk Institute and March of Dimes Chair in Molecular and Developmental Biology. R.M.E. is supported by grants from the Howard Hughes Medical Institute and the NIH (National Institute of Diabetes and Digestive and Kidney Diseases, and Nuclear Receptor Signaling Atlas). J.M.O. is supported by NIH grants and a University of California Discovery BioStar grant with matching funds from Pfizer Incorporated. S.J.F. is supported by grants from the Burroughs Wellcome Fund, the V Foundation, and the NIH.

Author Contributions X.Y. conceived the project, designed and performed most of the experiments. P.P.O. and S.J.F. participated in protein–lipid binding and cell imaging experiments. P.D.M. performed hyperinsulinaemic–euglycaemic glucose clamp studies. J.C.H. assisted in biochemical and animal experiments. F.Z. performed OGT activity assays. W.V.S. performed bioinformatic analyses. J.M.O., R.H.M., J.E.K. and S.J.F. provided intellectual input and technical expertise. R.M.E. supervised the project. X.Y. and R.M.E. wrote the manuscript.

Author Information Reprints and permissions information is available at www.nature.com/reprints. The authors declare competing financial interests: details accompany the full-text HTML version of the paper at www.nature.com/nature. Correspondence and requests for materials should be addressed to R.M.E. (evans@salk.edu).

METHODS

Plasmids. Vectors for bacterial expression of the full-length and deletion mutants of OGT in fusion with glutathione *S*-transferase (GST) were described previously[20]. Point mutants of OGT were generated with the QuikChange II site-directed mutagenesis kit (Stratagene). For expression of GFP fusion proteins, the wild-type and the KK/AA mutant of OGT were subcloned into pEGFP-C1 (Clontech).

Adenoviruses. Wild-type and KK/AA OGT, control GFP adenoviruses were generated with the pAd-easy system[43]. Inserts were cloned into the pAdTrack-CMV shuttle vector. Adenoviral constructs were created by recombination of the shuttle vector and pAdEasy vector by electroporation into BJ5183-AD-1 bacteria (Stratagene).

Protein–lipid binding assays. Protein–lipid overlay assays were performed with wild-type and mutant GST–OGT fusion proteins produced in *Escherichia coli* and PIP strips or PIP arrays purchased from Echelon Biosciences, in accordance with the manufacturer's protocols. PIP-affinity bead pulldowns were performed as described[44].

Cell culture, transfection, adenovirus infection, and treatment. Fao hepatoma cells were maintained in RPMI 1640 medium with 10% FBS. 3T3-L1, 3T3-A14 and COS-7 cells were cultured in DMEM medium with 10% FBS. 3T3-L1 cell differentiation was induced as described[45]. 3T3-A14 and COS-7 cells were transfected with Transfectin (Bio-Rad) and FuGENE6 (Roche), respectively. Where indicated, cells were infected with adenovirus in medium containing 0.5% BSA. Treatments with various concentrations of glucose and 100 μM PUGNAc were performed in 0.5% BSA for 16 h, followed by stimulation with 100 nM insulin. Where indicated, 50 mM LY294002 was added 30 min before stimulation with insulin.

Microscopy. Cells expressing fluorescent fusion proteins were fixed in 3.7% formaldehyde, mounted with DAPI-containing medium (Vectashield) and revealed with a TCS SP2 confocal microscope (Leica). The subcellular localizations of fluorescent fusion proteins were quantified by counting at least 50 cells in at least four randomly selected fields of view in each of three independent experiments. Live cell imaging was performed on an Olympus IX-81 DSU spinning-disk microscope with ZDC zero-drift autofocus. For dual-colour imaging a linear unmixing algorithm was applied to deconvolve the GFP and YFP data sets.

Subcellular fractionation. The experiment was performed as described[46].

Immunoprecipitation and immunoblotting. Whole-cell lysates were prepared with RIPA buffer. Lysates (400 μg) were immunoprecipitated with anti-IR-β and anti-IRS1 antibodies (Upstate). For anti-*O*-GlcNAc immunoprecipitation, CTD110.6 antibody (Covance) was covalently conjugated to anti-IgM as described[30]. Immunoblotting was performed as described[47].

***In vitro* kinase assays.** Non-radioactive Akt and ERK1/2 kinase assays were performed in accordance with the manufacturer's protocols (Cell Signaling).

Animals. Male 12-week-old C57BL/6J mice were maintained on a 12 h/12 h light/dark cycle and fed *ad libitum*. Recombinant adenovirus (5×10^8 plaque-forming units) was delivered by systemic tail-vein injection to mice anaesthetized with isoflurane. To measure metabolic parameters and liver gene expression, blood and the livers were collected from 6-h-fasted mice 7 days after viral infection. To assess signalling protein phosphorylation, 6-h-fasted mice were injected intraperitoneally with insulin (3 U kg^{-1} body weight) or vehicle. All indicated tissues were collected in liquid nitrogen 15 min after injection.

Glucose and insulin tolerance tests. At 4–6 days after viral infection, mice fasted for 6 h were injected intraperitoneally with glucose (1.5 g kg^{-1} body weight) or insulin (1.5 U kg^{-1} body weight). Blood glucose was measured from tail-vein blood collected at the designated times.

Hyperinsulinaemic–euglycaemic glucose clamp studies. Clamps were performed in 16-week-old C57BL/6J male mice 5 days after viral injection. The surgery to implant catheters and the glucose clamp method are described elsewhere[48] with the following modifications: surgery was conducted under isoflurane anaesthesia and insulin was infused at 3 mU kg^{-1} min^{-1}.

Measurement of metabolic parameters. Blood glucose was monitored from tail-vein blood with an automatic glucose monitor (One Touch; Lifescan). Plasma triacylglycerol, total cholesterol and non-esterified fatty acid levels were measured enzymatically with triacylglycerol GPO-Trinder, Infinity Cholesterol (Sigma) and NEFA C (Wako) reagents, respectively. Plasma insulin, leptin, adiponectin and resistin were measured with enzyme-linked immunosorbent assay kits (Linco). C-peptide was measured with an enzyme-linked immunosorbent assay kit (Wako). Liver triacylglycerol and glycogen contents were determined as described[49,50].

Quantitative PCR. Total RNA was extracted from mouse liver using TRIzol reagent (Invitrogen). Complementary DNA was synthesized from total RNA with Superscript II enzyme and random hexamer primers (Invitrogen). cDNAs were amplified with a SYBR green PCR kit and an ABIPRISM7700 detection system (Perkin Elmer). All data were normalized to the expression of 36B4 mRNA. Primer sequences are available from the authors on request.

43. Ongusaha, P. P. *et al.* p53 induction and activation of DDR1 kinase counteract p53-mediated apoptosis and influence p53 regulation through a positive feedback loop. *EMBO J.* **22,** 1289–1301 (2003).
44. Krugmann, S. *et al.* Identification of ARAP3, a novel PI3K effector regulating both Arf and Rho GTPases, by selective capture on phosphoinositide affinity matrices. *Mol. Cell* **9,** 95–108 (2002).
45. Furukawa, N. *et al.* Role of Rho-kinase in regulation of insulin action and glucose homeostasis. *Cell Metab.* **2,** 119–129 (2005).
46. Joost, H. G. & Schurmann, A. Subcellular fractionation of adipocytes and 3T3–L1 cells. *Methods Mol. Biol.* **155,** 77–82 (2001).
47. Su, K., Yang, X., Roos, M. D., Paterson, A. J. & Kudlow, J. E. Human Sug1/p45 is involved in the proteasome-dependent degradation of Sp1. *Biochem. J.* **348,** 281–289 (2000).
48. Miles, P. D., Barak, Y., He, W., Evans, R. M. & Olefsky, J. M. Improved insulin-sensitivity in mice heterozygous for PPAR-γ deficiency. *J. Clin. Invest.* **105,** 287–292 (2000).
49. Suzuki, Y. *et al.* Insulin control of glycogen metabolism in knockout mice lacking the muscle-specific protein phosphatase PP1G/RGL. *Mol. Cell. Biol.* **21,** 2683–2694 (2001).
50. Norris, A. W. *et al.* Muscle-specific PPARγ-deficient mice develop increased adiposity and insulin resistance but respond to thiazolidinediones. *J. Clin. Invest.* **112,** 608–618 (2003).